

Supplementary Information

Experimental supplementary information

Bacterial culture and imaging.

Inoculation of *P. vortex* bacteria on MH agar at 0.4-1% (w/v) resulted in the initiation of swarming motility within 1–8 hours when incubated at temperatures from 25 to 37°C. Imaging of swarming bacteria was performed by transmission light microscopy in a controlled environment, as described in more detail in the SI Methods.

Imaging

Imaging was performed by transmission light microscopy using an Olympus BX51 microscope with a total magnification of 40–500 fold (Olympus, Japan). A heated microscope stage (Marzhauser, Germany) was used to incubate plates during real-time imaging. Video was taken by F-View II CCD camera (Olympus, Japan) with resolution of 1376X1032 pixels. Frame rate was between 1 to 10 frames per second and the length of the movies was between 30 to 200 seconds. Most of the movies were taken with a 200 fold magnification, resulting in images that contain one or two branches.

The height of the microbial colonies was determined by focusing between the top and bottom (agar) using a x50 lens (Olympus, Fluorotar) with a low depth of focus (<200 nm) in conjunction with a Z axis control. Imaging and tracking cell movement used x4 and x10 dry lenses (Fluorotar, Olympus) with a depth of focus of 1.4 and 3.7 microns, respectively.

Measurement of nutrient depletion

In order to assess the nutrient depletion within *P. vortex* swarming colonies the bacteria were cultured on Mueller Hinton agar (Mueller Hinton broth from Oxoid, UK solidified with 1% w/v Eiken agar, Eiken Japan) in 9 cm diameter Petri dishes. Mueller Hinton agar contains starch which *P. vortex* can utilize as a carbon source. At different time points

(from 0 to 24 h with growth at 37 °C) the starch composition of the plate was assessed by staining with iodine vapor. This was done by scattering 200 mg iodine crystals (Sigma, NL) evenly within the inverted lid of the petri dish and incubating the agar plate, also inverted, over the lid for one hour at room temperature. Staining of the starch with iodine indicated that the macroscopic swarming colony depleted the starch over a period of 4 to 18 hours, particularly within the colony center. Therefore, there is a nutrient gradient across the swarming colony with the bacteria at the periphery having greatest access to starch; with this resource depleted > 200 fold at the colony center compared to the edge.

Image analysis. An image analysis algorithm was designed to process the imaging results, and was executed on Matlab. The algorithm maximizes local correlation between subsequent frames on a coarse grained grid with a regularizing penalty [S2].

Modeling and simulation supplemental information

Simulations.

Simulations were written and executed in Matlab, typically with 350 agents whose orientations and locations are updated synchronously at constant time intervals. The closed curve γ is simulated using an interface tracking method in which virtual agents model a dynamical discretization of the curve. The number of virtual boundary agents was adjusted on the fly to optimize the accuracy and efficiency of the discretization. Accordingly, virtual agents are added and eliminated in order to maintain the local concentration of agents per unit length approximately constant. Simulations were performed for several thousand steps until the system reached a steady state and the effect of initial conditions could not be observed.

Simulation details

The motion of a single agent. As explained in the main text, groups of several hundreds of bacteria are modeled as circular particles (agents) with radius $r = 0.65$, which corresponds to about $10 \mu m$. Denoting the position and velocity of agent i by x_i and v_i , respectively, the dynamics of a solitary agent is given by

$$\frac{dx_i}{dt} = v_i, \quad \frac{dv_i}{dt} = \Omega_i (v_{\max} - |v_i|) \hat{v}_i,$$

$$\Omega_i = c_e |\nabla n(x_i)|$$

In simulations, $v_{\max} = 1$ and $c_e = 1$. This ordinary differential equations is solved with the forward-Euler method with a step size of $\tau = 0.18$. Recall that a unit time in simulation corresponds to about 3 secs, i.e., each simulation step is about 0.55secs and $v_{\max} = 1$ corresponds to $5 \mu m / \text{sec}$, which is consistent with the experimentally observed speed of bacteria.

In principle, the rate for reaching the asymptotic speed, $\Omega_i = c_e |\nabla n(x_i)|$, may include a constant term, $\Omega_i = c_0 + c_e |\nabla n(x_i)|$ so that the rate does not vanish even if the gradient does. As this situation does not happen in our simulation setups, we found that adding the extra parameter c_0 does not qualitatively change simulation results and hence, for simplicity, set it to zero.

Interaction between modeled agents. The interaction between agents is detailed in the main text. Simulation parameters are $\alpha = 0.5$ and $\beta = 0.25$. Averages are taken for agents within $r_{\text{int}} = 3r$ of agent i . In addition, agents undergo inelastic collisions at a distance corresponding to a radius of $r = 0.65$ with a restitution coefficient of $\epsilon = 0.02$ (i.e., collisions preserve momentum but 0.02 of the total kinetic energy is lost).

More precisely, when particles i and j collide, denote by v_i and v_j their pre-collision velocities and by \tilde{v}_i and \tilde{v}_j their post-collision densities. Then,

$$\begin{aligned}
v_i + v_j &= \tilde{v}_i + \tilde{v}_j \\
(1 - \epsilon)v_i^2 + v_j^2 &= \tilde{v}_i^2 + \tilde{v}_j^2
\end{aligned}$$

Interaction with the envelope. Agents within a boundary layer up to a distance $r_{\text{env}} = 2$ from the envelope apply a force on the envelope. As explained in the text, the speed of points on the curve in the direction normal to is given by (5)

$$\frac{d\gamma_n(t; s)}{dt} = \left[C_\gamma \gamma_n \left(\sum_{|x_i - \gamma(s)| \leq r_{\text{env}}} \hat{v}_i \times [v_i \times \nabla n(\gamma(t; s))] \right) - \left(\sigma \kappa(s) + f_k \left| \frac{d\gamma_n}{dt} \right| + f_s \right) \right]_+,$$

where $\kappa(s)$ is the curvature of γ at s and $[\cdot]_+ = \max\{\cdot, 0\}$, $\sigma = 0.5$ is the surface tension coefficient, $f_k = 3$ and $f_s = 3$ are kinetic and static friction coefficients, respectively and $C_\gamma = 2.7$ a forcing coefficient.

Boundary condition. Agents are simulated up to a fixed length from the tip of the branch (about 100). Agents who leave this region are reintroduced at a random position.

Initial condition. The initial width of the branch is 20 (about $300 \mu\text{m}$). Initially, 70% of all agents are distributed uniformly inside the branch with a velocity that conforms to three-lane dynamics. Thus, simulations show that two and three-lane dynamics are a stable (or at least meta-stable) state of the dynamics. The rest of the agents are gradually introduced during the simulation.

Comparison between simulations and experiments

In order to quantify the dynamics inside a branch, we used image analysis and two dimensional measures: velocity profiling, vorticity, as discussed in the main text, and local order parameter.

- The velocity field $(u(x, y), v(x, y))$ is defined on a fixed spatial grid. In experiments, the optical flow between consecutive frames in the experimental

videos is obtained using the Horn-Schunk algorithm [S2]. The pattern is averaged onto a coarser grid. In simulations, the average velocity at a grid point is given by a local in time average of the velocity of all agents which are within a fixed distance (about $3r$) from the grid point.

- The vorticity field is given by $v(x, y) = \frac{\partial v}{\partial x} - \frac{\partial u}{\partial y}$.
- Let $(\bar{u}(x, y), \bar{v}(x, y))$ denote a vector field obtained by local averages (average over nearest neighbors) of (u, v) . The order parameter $\phi(x, y)$ is given by

$$\phi(x, y) = \frac{(u \cdot \bar{u} + v \cdot \bar{v})}{\sqrt{(u^2 + v^2) \cdot (\bar{u}^2 + \bar{v}^2)}}.$$

This allowed a quantitative comparison between the traffic organization in three lanes and in two lanes as well as in the experiments and in the simulations. We measured the flux and the vorticity through seven horizontal cuts in the branch and found a close similarity between the measurements in one instance of an experiment and a simulation both in three and in two lane formation (Figs. 3 and SI3). In order to compare the simulation with the experiments, all simulation units were rescaled to experimental ones as described above. We found a large difference in the local order parameter between three and two lane formation both in the experiment and in the simulation and a close similarity between the experiment and the simulation instances (Fig. SI4). We further measured the change in the branch area, width, advancement and the individual agents' average speed over time (Fig. SI5). We found consistent behavior between experimental instances, as discussed in the main text and close agreement with the simulation results. The area of the branch increases over time in all instances corresponding with momentarily increases in the branch width, which remains constant on average, combined with the advancement of the branch. The branch advancement increases with time while the individual average speed remains almost constant, showing very close agreement between the experimental instances and the simulation instances after

normalization. Advancement is higher for three lane formation, both in experiments and simulation.

The effect and sensitivity of the model parameters

We made a thorough investigation of the effect of the model parameters on the observed simulated dynamics. In addition of a qualitative examination of the general characteristic such as mainlining a constant branch width and stability of the envelope, we measured the effect of changes in parameters on three macroscopic observables which were found to be compatible with experimental values

- The probability of three vs. two lane formations.
- The average advancement speed of the branch when moving.
- The average speed of agents.

Fig. SI6 shows results in the variation of

1. The number of agents, N .
2. The static friction coefficient, f_s .
3. The surface tension, σ .
4. The maximum speed of individual agents, v_{\max} .
5. The forcing coefficient, C_γ .

Except for the forcing coefficient, we found that there exists a wide range for which small changes do not affect the model behavior.

- The number of agents: Changing the number of agents does not directly correspond to a different bacterial concentration in experiments. The interaction between cells is highly dependent on the local concentration. As a result, the both effective behavior of single agents as well as the effective agent-agent interactions may be completely different at different bacterial or food concentrations. None the less, from the modeling point of view it is important to consider the simulated dynamics at different concentration.

Decreasing the number of agents below a threshold (250) leads to no advancement of the branch due to insufficient forces to overcome the static friction. A high number of agents (over 550) leads to a smoother motion almost exclusively in three lanes for the opposite reason. The intermediate range for the number of agents where the behavior of the model remains coherent is 300-500, where the default value used in the simulations is 350.

- Static friction is the minimal force agents need to apply so that the envelope will start moving. The range where the model remains coherent is 2-5 where the default value used in the simulation was 3. Very low static friction (under 1) leads to a very fast advancing branch which even becomes thinner due to its speed. We a high static friction (over 8), the branch cannot move.
- Surface tension: We found a wide range with no significant effect. However, with high values there is no advancement and for small values the envelope becomes unstable, which is expected as small perturbations in curvature are not attenuated.
- The maximum individual agent speed effectively determines average speed of agents Moreover, above a certain threshold, the branch speed increases with the maximum speed. The reason is that the effective force agents apply on the envelope is proportional to the speed of the agents. There is an intermediate range, 0.9-1.8, for which the behavior of the model is consistent with experiments and both two and three lane formation exist. The default value used is 1.
- Kinetic friction is a drag force slowing down the envelope as it advances. There is an intermediate range (1-3.5, default is 3.5) where the behavior of the model remains coherent. For smaller values (under 0.5), the envelope becomes unstable and develops irregularities. For larger values (over 4) the envelope slows down until it stops moving.
- The forcing coefficient, C_γ : This is the main term through which agent influence the envelope and results are highly sensitive to its value. There is an intermediate range (2-2.7, default is 2.7) for which the behavior is coherent

and consistent with experimental results. For smaller values the envelope does not advance while for higher values the branch expands in all directions.

While reviewing the model, other choices for mechanistic solutions may arise in one's mind, some of these will lead to very similar results while some will require extensive fine tuning, and some are statistically similar to the choices we have made. There is a large amount of such possible mechanisms, in our attempts we have found one.

We emphasize that the model provides a representation of the reality. The model parameters, including their sizes and strengths, have a different meaning and effect than the physical parameters of the experiments, although they might have similar names. For example, the number of agents in the model has a very different meaning than the number of bacteria in an experiment. In the simulation, the number of agents affects the coarse graining of the simulation into groups which affects the strengths of interaction with the envelope. The reason for this mismatch is that the model was built to approach the minimal representation of a complicated setting of which much is unknown: the nature of the lubricant, its effect on the bacteria, and the exact forces between the bacteria among other critical information.

Figures

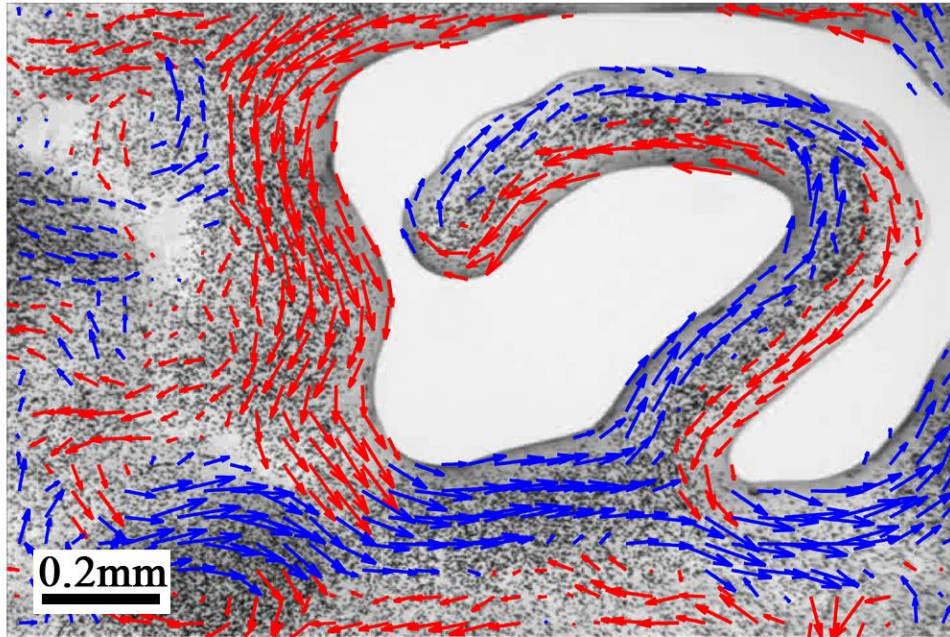


Figure S11. A zoomed view showing the internal dynamics around a single compartment and a branch. The figure shows the velocity field of micrometer beads (dark dots) that are transported and carried by bacteria. Colors represent projection into the bottom-left (red) or to-right (blue) directions. The motion consists of vortices and stable traffic lanes made of cells advancing in a tight formation and mixing across the colony. This swarming logistics allows transportation of cargo through the colony including nutrients, spores and even other organisms. The snapshot is taken from Movie S11.

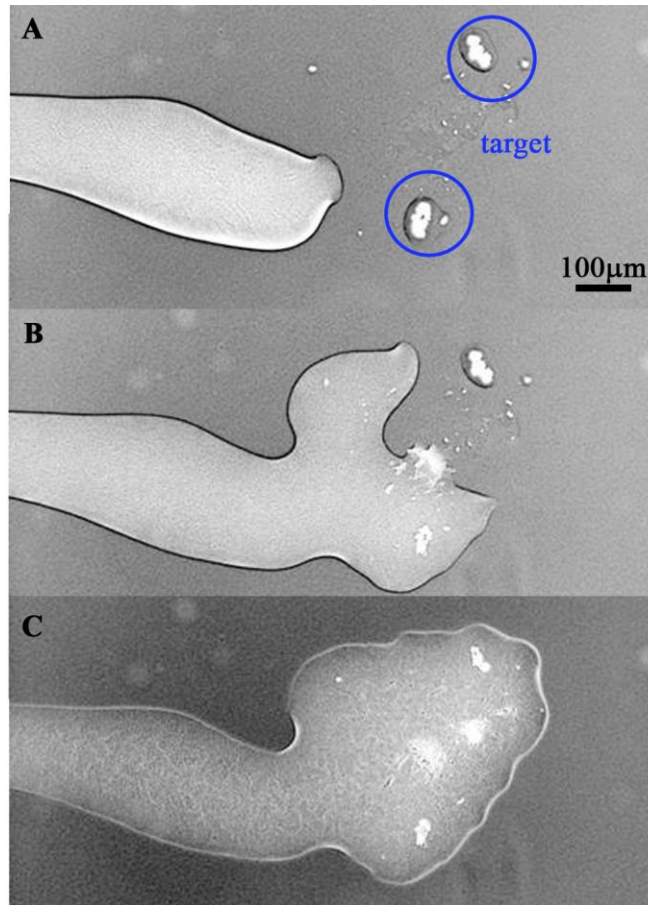


Figure SI2. A swarm navigates and splits towards two sources of nutrients (blue circles). Light microscopy of *P. vortex* moving on MH agar (0.3% w/v), extending into an area where extracellular material derived from washes of swarming cells was delivered by toothpick and allowed to soak into the agar. Dark marks inside the area of the extract are disturbances due to the toothpick contacting the agar. The cell mass starts to disperse as it contacts the area of the extract (top). After six seconds, the cell mass splits to cover the two sources (middle). After eight more seconds, the cell mass has dispersed into the area of the extract and additional cells are moving into this area from further back in the colony (bottom). Image reproduced with permission from [S1].

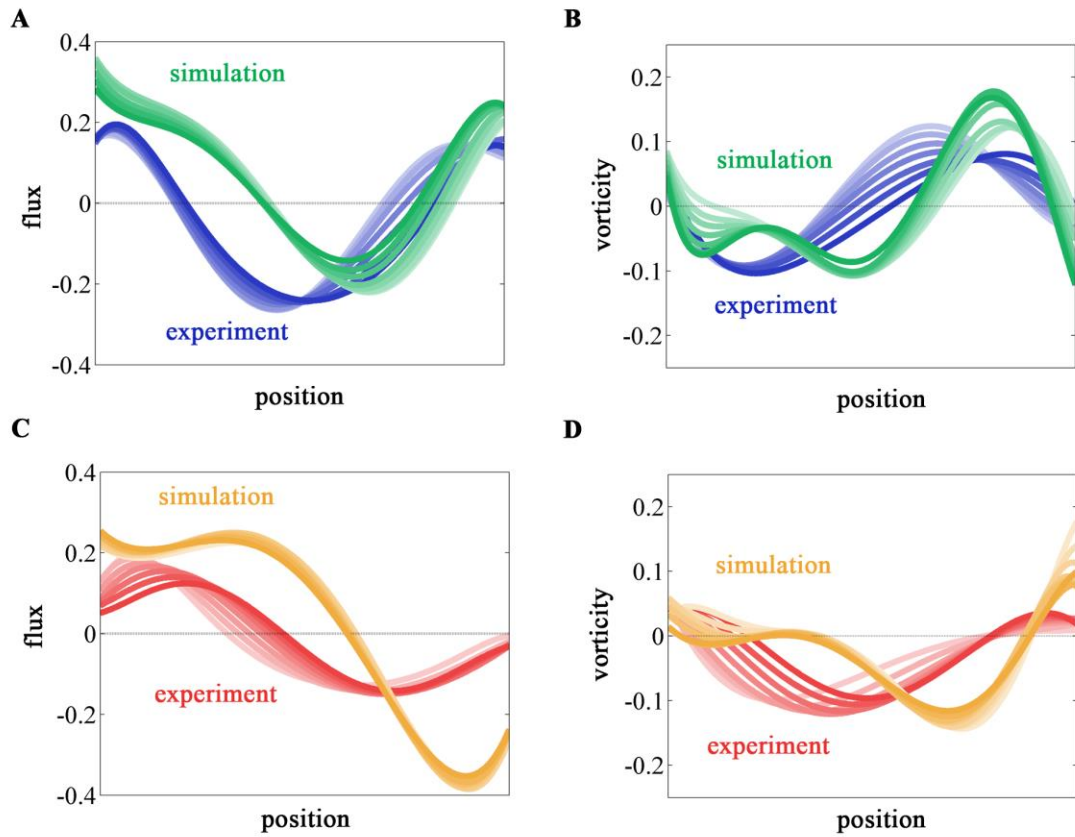


Figure SI3. Comparison between experiment and simulation. Comparison of measurements along seven horizontal cuts across a branch in an experiment (dark blue and red) and a simulation (green and yellow). The figure shows the flux (left) and vorticity (right) in three (top) and two (bottom) lane formations. Simulation values were scaled in order to fit experiment values as explained in the SI section.

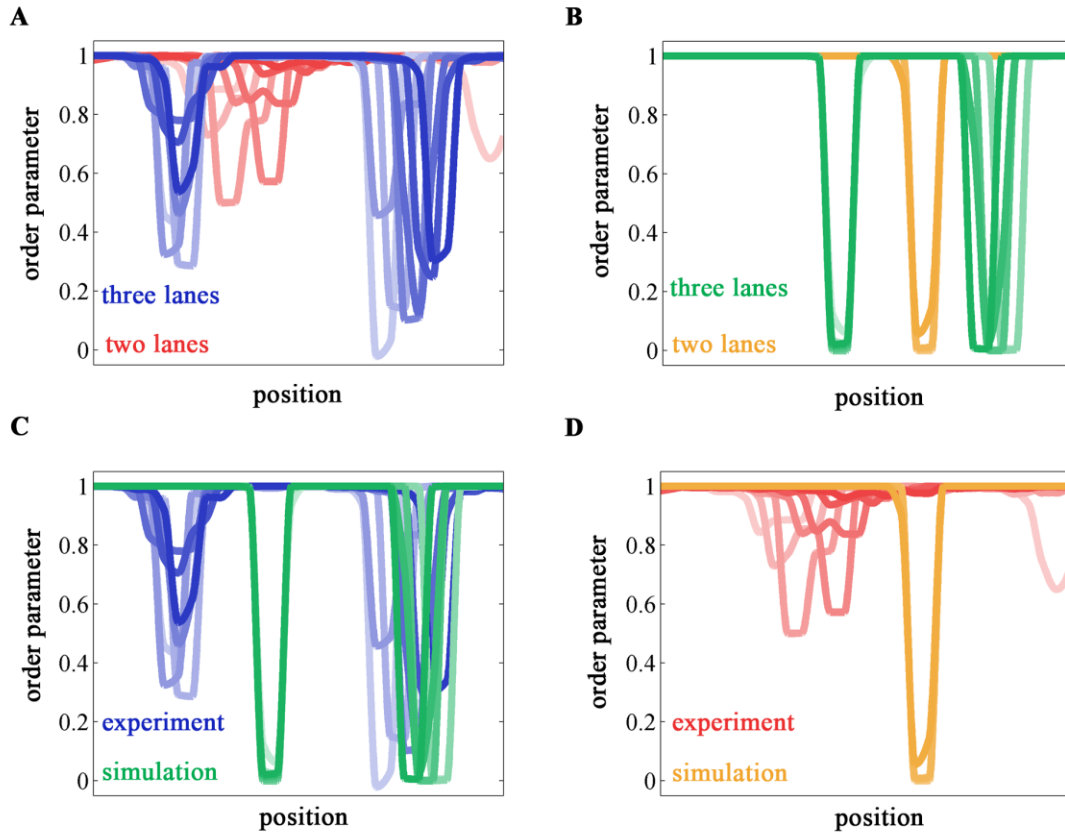


Figure S14. Local order parameter. Comparison of the local order parameter along seven horizontal cuts across a branch in three and two lane formation in an experiment (dark blue and red) and a simulation (green and yellow). The figure shows comparison between two and three lanes (top) in an experiment (left) and a simulation (right) and comparison between experiment and simulation (bottom) in three lane formation (left) and two lane formation (right).

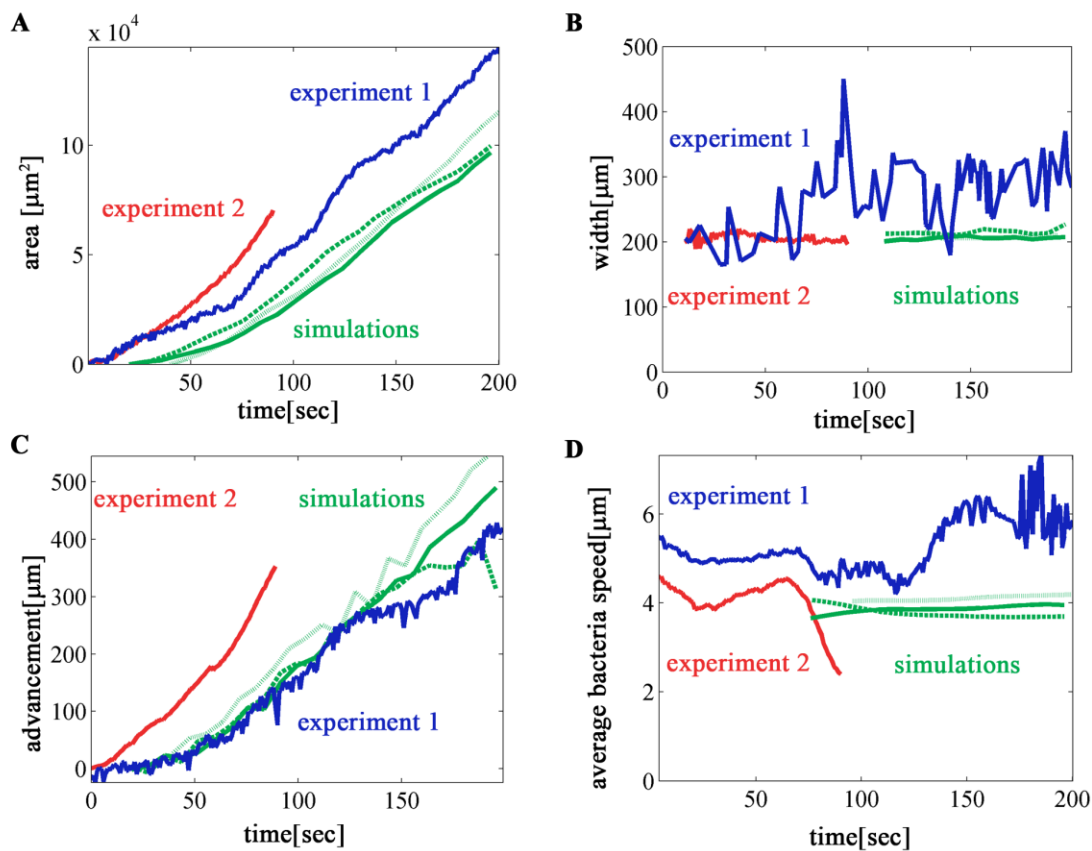


Figure SI5. Comparison of the swarm dynamics in experiment and simulation. The figure shows details of the dynamics of the swarm and the edge of the lubricating fluid it produces. Blue: the experimental movie SI2 (also Fig 2A). Red: the experimental movie SI3 (also Fig 2D). Green: three simulation instances -movie SI5 (solid line), movie SI7 (dashed line), and movie SI8 (dotted line).

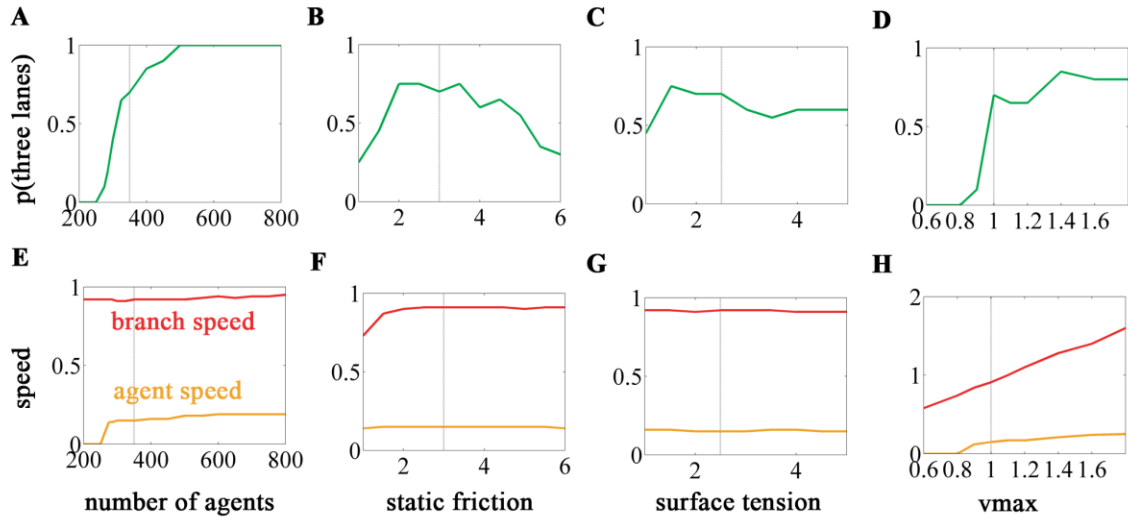


Figure SI6. The effect and sensitivity of the model to parameters – (A) number of agents, (B) static friction, (C) surface tension, and (D) maximum agent speed. The measurements include the probability of three lane formation (vs. two lanes) and the speed of an individual agent (red) and the branch (yellow).

Movie Legends

Movie SI1. Experiment. The internal dynamics around a single compartment and a branch. The figure shows the velocity field of micrometer beads (dark dots) which are transported and carried by bacteria. Colors represent direction. The motion consists of vortices and stable traffic lanes made of cells advancing in a tight formation and mixing across the colony. This swarming logistics allows transportation of cargo through the colony including nutrients, spores and even other organisms.

Movie SI2. Experiment. The velocity field showing the swarm dynamics inside a moving branch.

Movie SI3. Experiment. The velocity field showing the swarm dynamics inside a branch which is being repelled from a neighboring one.

Movie SI4. Experiment. The velocity field showing the progression of a branch which is being repelled from a neighboring one.

Movie SI5. A simulated branch moving in a nutrient field with a constant gradient showing three-lane traffic.

Movie SI6. A simulated branch moving and then stopping in a nutrient field with a constant gradient showing two-lane traffic.

Movie SI7. A simulated branch moving in the effective field of a neighboring branch.

Movie SI8. A simulated branch moving towards a source.

Movie SI9. A simulated branch moving and splitting towards two sources.

Supplementary Information References

- S1. Ingham CJ, Ben-Jacob E (2008) Swarming and complex pattern formation in *Paenibacillus* vortex studied by imaging and tracking cells. *BMC Microbiol* 8:36.
- S2. Horn BKP, Schunck BG (1981) Determining optical flow. *Artif Intell* 17:185–203.